doi:10.1093/brain/awv350 BRAIN 2016: 139; 346–354 | 346

BRAIN
A JOURNAL OF NEUROLOGY

REPORT

Human thioredoxin 2 deficiency impairs mitochondrial redox homeostasis and causes early-onset neurodegeneration

Eliska Holzerova,[1,2] Katharina Danhauser,[3] Tobias B. Haack,[1,2] Laura S. Kremer,[1,2] Marlen Melcher,[3] Irina Ingold,[4] Sho Kobayashi,[4,5] Caterina Terrile,[2] Petra Wolf,[2] Jörg Schaper,[6] Ertan Mayatepek,[3] Fabian Baertling,[3] José Pedro Friedmann Angeli,[4] Marcus Conrad,[4] Tim M. Strom,[2] Thomas Meitinger[1,2,7] Holger Prokisch[1,2,*] and Felix Distelmaier[3,*]

*These authors contributed equally to this work.

Thioredoxin 2 (TXN2; also known as Trx2) is a small mitochondrial redox protein essential for the control of mitochondrial reactive oxygen species homeostasis, apoptosis regulation and cell viability. Exome sequencing in a 16-year-old adolescent suffering from an infantile-onset neurodegenerative disorder with severe cerebellar atrophy, epilepsy, dystonia, optic atrophy, and peripheral neuropathy, uncovered a homozygous stop mutation in *TXN2*. Analysis of patient-derived fibroblasts demonstrated absence of TXN2 protein, increased reactive oxygen species levels, impaired oxidative stress defence and oxidative phosphorylation dysfunction. Reconstitution of TXN2 expression restored all these parameters, indicating the causal role of *TXN2* mutation in disease development. Supplementation with antioxidants effectively suppressed cellular reactive oxygen species production, improved cell viability and mitigated clinical symptoms during short-term follow-up. In conclusion, our report on a patient with TXN2 deficiency suggests an important role of reactive oxygen species homeostasis for human neuronal maintenance and energy metabolism.

1 Institute of Human Genetics, Technische Universität München, Trogerstr. 32, 81675 Munich, Germany
2 Institute of Human Genetics, Helmholtz Zentrum München, Ingolstädter Landstr. 1, 85764 Neuherberg, Germany
3 Department of General Paediatrics, Neonatology and Paediatric Cardiology, University Children's Hospital, Heinrich-Heine-University Düsseldorf, Moorenstr. 5, 40225 Düsseldorf, Germany
4 Institute of Developmental Genetics, Helmholtz Zentrum München, Ingolstädter Landstr. 1, 85764 Neuherberg, Germany
5 Division of Animal Production, Specialty of Bioproduction Science, The United Graduate School of Agricultural Sciences, Iwate University, Morioka, Iwate 020-8550, Japan
6 Medical Faculty, Department of Diagnostic and Interventional Radiology, University Düsseldorf, Moorenstr. 5, 40225 Düsseldorf, Germany
7 Munich Cluster for Systems Neurology (SyNergy), 80336 Munich, Germany

Correspondence to: Holger Prokisch,
Institute of Human Genetics,
Technische Universität München,
Trogerstr. 32,
81675 Munich, Germany
E-mail: prokisch@helmholtz-muenchen.de

Received May 21, 2015. Revised August 18, 2015. Accepted October 15, 2015. Advance Access publication December 1, 2015

Correspondence may also be addressed to: Felix Distelmaier,
Department of General Paediatrics,
Heinrich-Heine-University,
Moorenstr. 5,
40225 Düsseldorf, Germany
E-mail: felix.distelmaier@med.uni-duesseldorf.de

Keywords: idebenone; mitochondria; neurodegeneration; ROS; thioredoxin

Abbreviation: CM-H_2DCFA = 5-(and-6)-chloromethyl-2′,7′-dichlorodihydrofluorescein diacetate; GSH = glutathione; OXPHOS = oxidative phosphorylation system; ROS = reactive oxygen species

Introduction

The umbrella term reactive oxygen species (ROS) comprises a wide array of partially reduced forms of oxygen, which are common by-products of cellular metabolism. Most intracellular ROS are derived from mitochondrial superoxide, which results from the monoelectronic reduction of oxygen (Zorov *et al.*, 2014; Holzerova and Prokisch, 2015). Superoxide is efficiently dismutated to hydrogen peroxide (H_2O_2) via superoxide dismutase, consequently making the mitochondria a major site for H_2O_2 generation. In this context, tight regulation of mitochondrial H_2O_2 levels is critical for their ability to participate in physiological cell signalling and to avoid non-specific oxidative damage (Sena and Chandel, 2012). Therefore, an efficient enzymatic machinery to buffer H_2O_2 levels has developed within the mitochondrial matrix (Fig. 1). Key proteins involved in these processes are members of the thioredoxin (TXN) and the glutathione (GSH) systems (Zhang *et al.*, 2007). The mitochondrial TXN system is composed of TXN2, thioredoxin reductase 2 (TXNRD2), peroxiredoxin 3 (PRDX3) and peroxiredoxin 5 (PRDX5) (Lu and Holmgren, 2012; Mahmood *et al.*, 2013). TXN2 is ubiquitously expressed with highest expression levels in the brain (Rybnikova *et al.*, 2000). It is encoded by a nuclear gene, *TXN2*, containing a mitochondrial targeting sequence. Along with TXNRD2 and PRDX3/5, TXN2 is responsible for eliminating H_2O_2, thus maintaining a reducing mitochondrial matrix environment (Lu and Holmgren, 2012). Moreover, TXN2 is involved in controlling the intrinsic-mitochondrial apoptotic pathway (Tanaka *et al.*, 2002; Lu and Holmgren, 2012). Animal studies suggest that TXN2 is essential for prenatal development as total absence of TXN2 in a mouse knockout model causes exencephaly and embryonic lethality (Nonn *et al.*, 2003).

In this study, we describe a 16-year-old adolescent suffering from early-onset neurodegeneration and severe cerebellar atrophy associated with a homozygous stop mutation

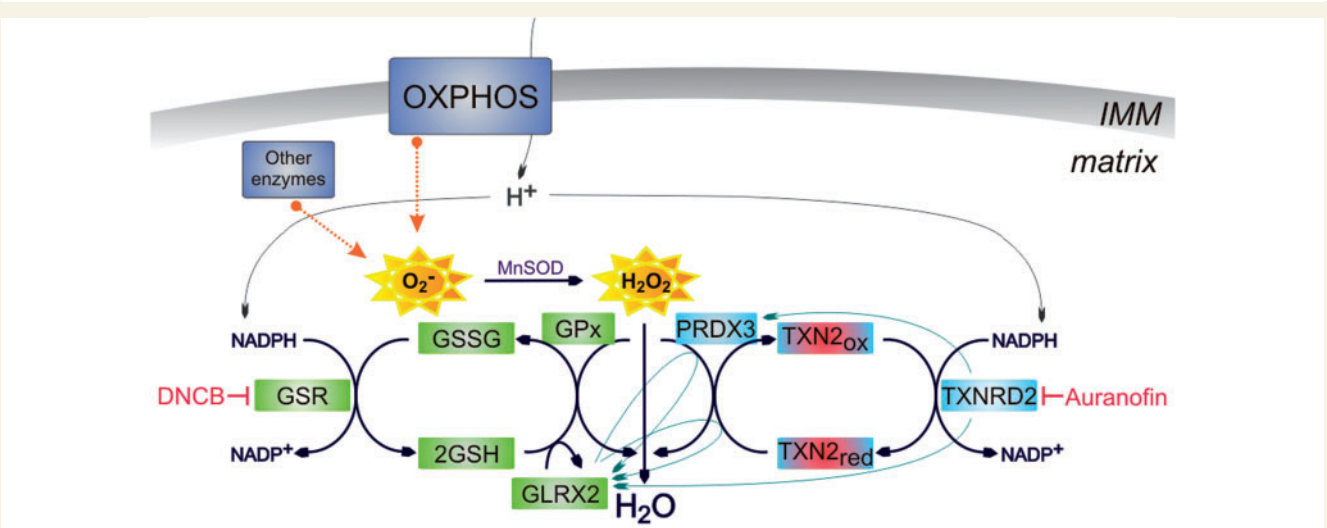

Figure 1 Function of TXN2 in the ROS defence system. The schematic representation of the ROS scavenging systems shows involved proteins in two crosslinked pathways within the mitochondrial matrix. Different proteins as well as complexes of the oxidative phosphorylation system (OXPHOS) produce reactive oxygen species in the form of superoxide (O_2^-), which spontaneously converts to hydrogen peroxide (H_2O_2), or with the help of manganese superoxide dismutase (MnSOD). Within mitochondria, H_2O_2 is sensed by PRDX3 and oxidation of PRDX3 is reduced by TXN2, which is highlighted in red due to a missing function. TXN2 is reduced by TXNRD2 and NAPDH. In the glutathione pathway, glutathione peroxidase (GPx) reduces H_2O_2 and is subsequently reduced by GSH molecules, which form dimers (GSSG) or by glutaredoxin 2 (GLRX2). Using NADPH, glutathione reductase (GSR) reduces dimers of GSH. Inhibitors of the systems are depicted in red. DNCB = 2,4-dinitrochlorobenzene; IMM = inner mitochondrial membrane.

in *TXN2*. This mutation causes impaired ROS homeostasis and secondary mitochondrial dysfunction.

Case report

The boy is the first child of healthy, non-consanguineous German parents. Prenatal ultrasound at 16 weeks gestation revealed bilateral subependymal cysts and brachycephaly but was otherwise normal. Chorion biopsy and foetal chromosome analysis were performed and revealed no abnormalities. The child was born at term without complications. Apart from primary microcephaly, no specific dysmorphic features or anomalies were seen. However, the parents noted that the child appeared relatively quiet and less active.

At the age of 6 months, he was severely microcephalic (head circumference 4 cm below third percentile) and showed reduced spontaneous movements. Brain MRI detected an abnormally increased T_2 signal intensity of the cerebellum and indicated global brain atrophy. In addition, abnormal hippocampal shape and bilateral subependymal cysts were seen (Fig. 2A–F). Lumbar puncture and analysis of CSF revealed elevated lactate (4.6 mmol/l, norm <2.8 mmol/l) and protein (67 mg/dl; norm <50 mg/dl) levels. In addition, blood lactate was moderately increased (up to 3.1 mmol/l, norm <1.6 mmol/l).

Follow-up at the age of 14 months revealed impaired psychomotor development characterized by markedly disturbed muscle tone and movement coordination. Brain MRI demonstrated a rapid progression of cerebellar atrophy and indicated delayed myelination. At the age of 22 months, a muscle biopsy with biochemical analysis of the oxidative phosphorylation system (OXPHOS) revealed reduced activities of mitochondrial complex I [56 mU/U citrate synthase (CS), norm 70–250 mU/U CS] and complex III (1500 mU/U CS, norm 2500–6610 mU/U CS) as well as a reduced global ATP production rate (9 mmol ATP/mU CS; norm 42–81 mmol ATP/mU CS), confirming a mitochondrial disorder.

The further clinical course was characterized by severely disturbed global development with a spastic-dystonic movement disorder. Starting from the age of 4 years, the boy developed severe, drug-resistant epilepsy. Feeding difficulties required placement of a percutaneous endoscopic gastrostomy. The patient developed a gastrointestinal motility disturbance most likely due to autonomic neuropathy. Clinical follow-up at the age of 12 years revealed severe optic neuropathy and retinopathy. Nerve conduction studies demonstrated peripheral neuropathy with axonal degeneration. Brain MRI findings are depicted in Fig. 2C, E and F. Magnetic resonance spectroscopy was without pathological findings. Lumbar puncture was repeated and again showed increased lactate and protein levels.

Material and methods

Sequencing

A DNA sample from the patient was sequenced by Whole Exome Sequencing using SureSelect Human All Exon 50 Mb V5 Kit (Agilent) on a HiSeq2500 system (Illumina) (Haack *et al.*, 2012; Kornblum *et al.*, 2013). The mutation was confirmed by Sanger sequencing in the patient's and parents' samples.

Drug sensitivity assay and antioxidant treatment

Human fibroblasts were cultured overnight on 96-well plate in Dulbecco's modified Eagle medium (DMEM), 10% foetal bovine serum, 1% penicillin-streptomycin, 200 µM uridine, ± antioxidants when indicated. On the following day, the cells were exposed to increasing concentrations of the indicated compounds dissolved in DMEM. Cell viability was determined by AquaBluer Kit (MultiTarget Pharmaceuticals LLC) after 72 h of cultivation.

Lentiviral gene rescue

The wild-type sequence of the *TXN2* gene was amplified from a control cDNA and cloned into pLenti6.3/V5-TOPO® TA Cloning® Kit (Invitrogen) for expression of *TXN2* in human fibroblasts (Kornblum *et al.*, 2013).

SDS PAGE and western blot analysis

Protein lysates were separated by sodium dodecyl sulphate polyacrylamide gel electrophoresis (SDS-PAGE) on 10–20% precast gels (LONZA). The polyvinylidene difluoride (PVDF) membranes were immunoblotted with antibodies against TXN2 (HPA000994, Sigma-Aldrich), β-actin (A5441, Sigma-Aldrich), SDHA (ab14715, Abcam) and a previously described self-made anti-peroxiredoxin-3 antibody (Godoy *et al.*, 2011).

Cell respiration

Oxygen consumption rate was measured using a XF96 Extracellular Flux Analyzer (Seahorse Biosciences). Oxygen consumption rate was determined without supplements (basal), after addition of oligomycin (1 µM), after addition of carbonyl cyanide-*4*-(trifluoromethoxy)phenylhydrazone (FCCP, 0.4 µM) and after addition of rotenone (2 µM) (Haack *et al.*, 2012).

Reactive oxygen species measurements

For measurements of global cellular ROS production, cells were seeded on 96-well plates (DMEM, low glucose, no

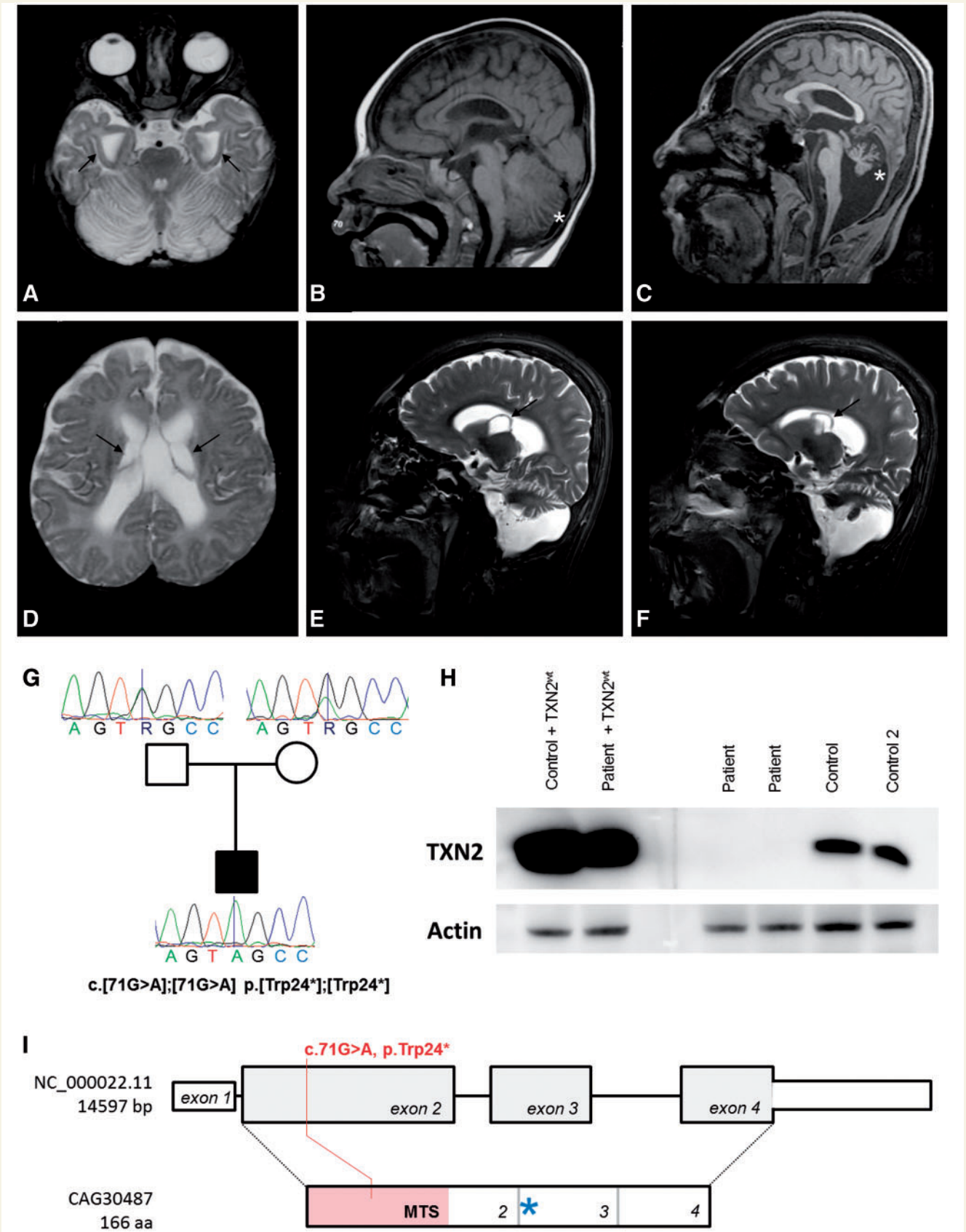

Figure 2 Brain imaging and genetic findings. (**A**) Brain MRI, T_2-weighted image, axial view at the age of 6 months demonstrating bilateral abnormal hippocampal shape (black arrows). Moreover, an abnormally increased T_2 signal intensity of the cerebellum is observed. (**B** and **C**) T_1-weighted images, sagittal view at the age of 6 months (**B**) and 12 years (**C**) showing the development of severe cerebellar atrophy (cerebellum

(continued)

phenol red). After 24 h, cells were washed with phosphate-buffered saline and incubated with 5-(and-6)-chloromethyl-2′,7′-dichlorodihydrofluorescein diacetate (CM-H_2DCFDA; 10 μM for 20 min) in HEPES-Tris medium (132 mM NaCl, 4.2 mM KCl, 1 mM $MgCl_2$, 5.5 mM D-glucose, 10 mM HEPES, 1 mM $CaCl_2$, pH 7.4). Kinetic fluorescence measurements were performed for 10 min (Tecan Infinite M200 Multiplate reader; excitation 485 nm, emission 520 nm). Values were normalized on cell count, which was quantified using a CyQuant® cell proliferation assay C7026 (Invitrogen).

Specific measurements of mitochondrial ROS levels were performed according to a modified protocol described previously (Distelmaier *et al.*, 2015). In brief, cells were cultured on glass bottom dishes (Greiner BioOne, CELLview™) in DMEM (low glucose, no phenol red) for 72 h. Next, cells were incubated with MitoSOX™ Red (5 μM, 10 min, 37°C; Invitrogen). Images were obtained using an Axiovert M200 microscope (Zeiss; 40 × objective) equipped with a dihydroethidium filter set (excitation: 500/24 BrightLineHC; emission: 595/50 H band-pass; Zeiss). Fluorescence intensity was quantified using ImageJ software (Wayne Rasband at the National Institutes of Health; http://rsbweb.nih.gov/ij/).

Whole cell ATP measurements

Cells were cultured on 96-well plates. Whole-cell ATP levels were determined using the PerkinElmer ATPlite assay system (6016941) according to the manufacturer's protocol. Values were normalized on cell count, which was quantified using a CyQuant® cell proliferation assay C7026 (Invitrogen).

Statistical analysis and experimental design

Two-tailed two-sample Student's *t*-test was followed to determine the statistical significance in Fig. 3 $*P < 0.05$; $**P < 0.01$; $***P < 0.001$, assuming a normal distribution. Error bars indicate standard deviation in Figs 3C and D, and 4 A and D and standard error of mean in Fig. 4B and C. All experiments were performed 4–20 times. For MitoSOX™ Red measurements between 157 and 218 individual living cells were analysed per condition.

Results

The mutation in *TXN2* causes a premature stop codon, resulting in the loss of TXN2 protein

Whole exome sequencing discovered a homozygous stop gain mutation in the *TXN2* gene c.[71G > A];[71G > A], p.[Trp24*];[Trp24*] in the patient's DNA. The non-consanguineous parents were identified as heterozygous carriers of the mutation (Fig. 2G). In 6800 exomes (in-house database) only the patient reported here presented with a bi-allelic variant. The Exome Aggregation Consortium lists 12 heterozygous loss-of-function alleles out of 120 000 analysed and no other homozygous rare coding variant. TXN2 starts with a mitochondrial targeting sequence of 59 amino acids and the p.Trp24* mutation is located therein (Fig. 2I). The next ATG codon is located after the active site. Using an anti-TXN2 polyclonal antibody we detected TXN2 in control fibroblasts and in fibroblasts with re-expressed wild-type *TXN2*, but we were unable to detect TXN2 in patient-derived cells (Fig. 2H).

TXN2 is essential for efficient cycling of PRDX3

TXN2 plays an important role in the mitochondrial H_2O_2 defence system by reducing peroxiredoxin dimers formed upon reaction with H_2O_2 (Fig. 3A), thereby keeping peroxiredoxins in their reduced and active state (Winterbourn and Hampton, 2015). Along with TXN2/TXNRD2, peroxiredoxins reacts catalytically with H_2O_2. A PRDX3 monomer first reacts with H_2O_2 through its peroxidatic cysteine, thus generating a sulphenic acid at the peroxidatic cysteine. The sulphenic acid condensates with a resolving cysteine from a second PRDX3 molecule, thus forming a homodimer linked via a disulphide (PRDX3 dimers).

Figure 2 Continued
is marked by asterisks). (**D**) T_2-weighted image, axial view at the age of 6 months demonstrating large bilateral subependymal cysts (black arrows). (**E** and **F**) T_2-weighted images, right (**E**) and left (**F**) parasagittal view at the age of 12 years, also depicting the bilateral subependymal cysts. (**G**) Homozygous mutation in a patient sample was confirmed by Sanger sequencing. Non-consanguineous parents are both heterozygous carriers of the mutation. (**H**) Total cell extracts from fibroblast cell lines were separated by SDS-PAGE and blotted on a PVDF membrane, which was labelled with anti-thioredoxin-2 (generated against 138 of 166 amino acids) and anti-β-actin antibodies and developed with different exposure times. No TXN signal was observed in the samples prepared from patient fibroblast cell line in contrast to control cell lines and after re-expression of *TXN2* in control and patient cell line (+ $TXN2^{WT}$). Both membrane scans interpret a representative selection of the whole image. (**I**) The homozygous mutation c.71 G > A causes a premature stop codon. The gene *TXN2* consists of four exons, of which exon 1 is not translated and exon 2 contains a predicted mitochondrial targeting sequence (MTS). TXN2 contains an active site (WCGPC, indicated by a blue asterisk) that is located at the very beginning of exon 3. The second in-frame ATG codon is located after the active site of the protein.

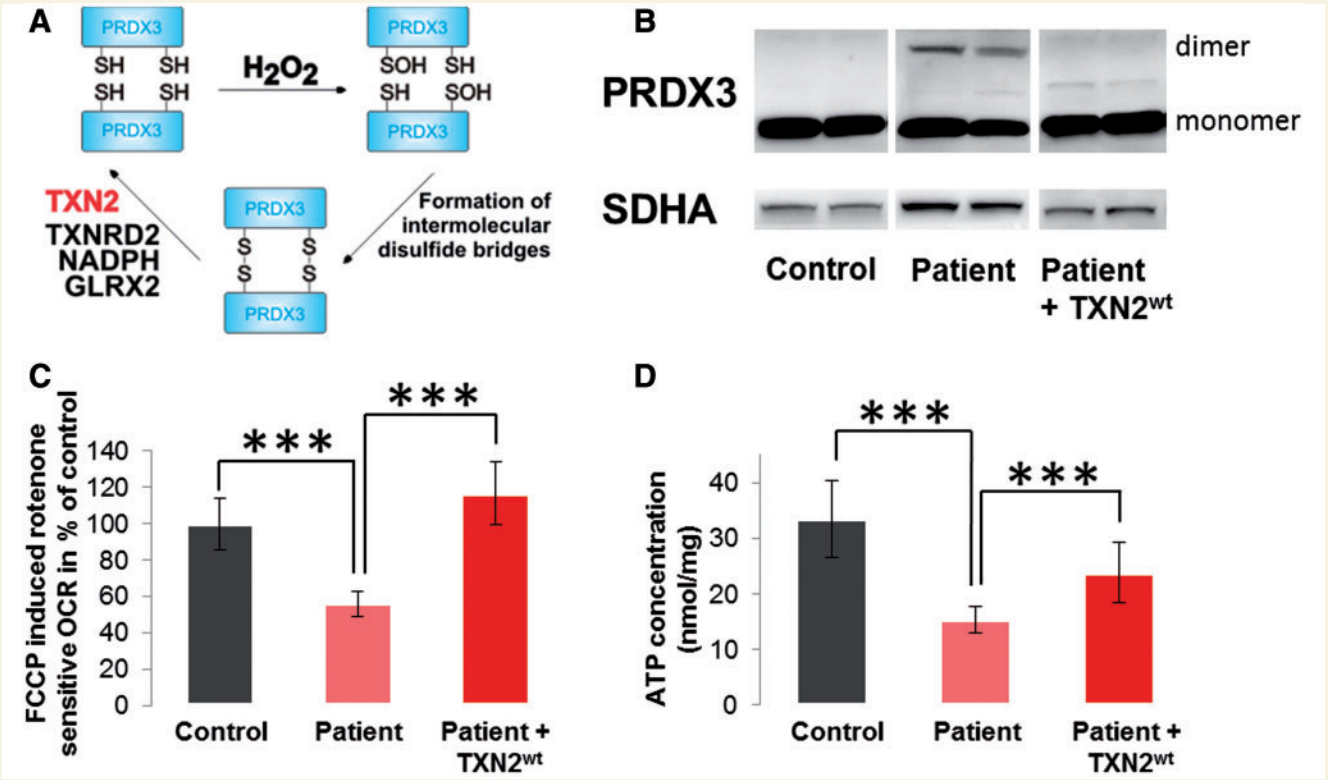

Figure 3 Cellular consequences of TXN2 deficiency. As indicated in scheme (**A**), TXN2 reduces PRDX3 dimers and restores the monomeric, active form. Missing function of TXN2 protein led to detectable amounts of PRDX3 dimers (**B**). Presented membrane scans interpret a representative selection of the whole image. Succinate dehydrogenase complex subunit A (SDHA) was used as a loading control. (**C**) FCCP-uncoupled induced, rotenone-sensitive oxygen consumption rate was analysed by XF96 Extracellular Flux Analyzer. Control values were set as 100%. Respiration of patient fibroblast was significantly reduced. Re-expression of *TXN2* rescued the respiratory function. (**D**) ATP production measured in whole cells revealed significant reduction in patient fibroblasts compared to control cells and cells with re-expressed *TXN2*. Values were normalized to protein content after measurement.

Here, we show that under standard growth conditions in control cell lines, the PRDX3 dimer could not be detected. By contrast, a substantial amount of PRDX3 was found in its dimeric state in the patient cell line, which was reduced to the monomeric form in patient cell line after re-expression of *TXN2* (Fig. 3B).

TXN2 deficiency impairs mitochondrial function

Investigation of cellular respiration in patient fibroblasts demonstrated only slightly reduced basal respiration rate as compared to control cells, while the maximal oxygen consumption rate in uncoupled mitochondria was significantly reduced by about half, accompanied by decreased ATP production (Fig. 3C and D). Supporting the importance of TXN2 in these processes, re-expression of *TXN2* normalized all parameters investigated. This suggests that a tight control of mitochondrial H_2O_2 levels is required to prevent dysfunction of the OXPHOS system. Of note, we observed neither any difference in the total cell concentration of glutathione, nor increased mRNA levels of known components of the ROS defence system as a consequence to TXN2 loss (data not shown).

TXN2 deficiency impairs cellular reactive oxygen species homeostasis

In view of the importance of TXN2 for oxidative stress defence, we measured global cellular ROS levels using the cell-permeable dye CM-H_2DCFDA. Of note, CM-H_2DCFDA is a widely used ROS indicator that reacts with different ROS species including hydrogen peroxide, hydroxyl radicals and peroxynitrite. Measurements revealed significantly increased ROS levels in patient fibroblasts under resting conditions (Fig. 4A, basal). In addition, to indicate the mitochondrial origin of increased ROS production, we performed measurements using the mitochondria-targeted superoxide indicator MitoSOX Red. In agreement with the CM-H_2DCFDA data, measurements showed highly increased ROS levels in the patient cell line (Fig. 4B). Next, we examined the sensitivity of patient cells towards pharmacological interference with the TXN and GSH system by analysing cell survival. Cells were treated for 72 h with different inhibitors of

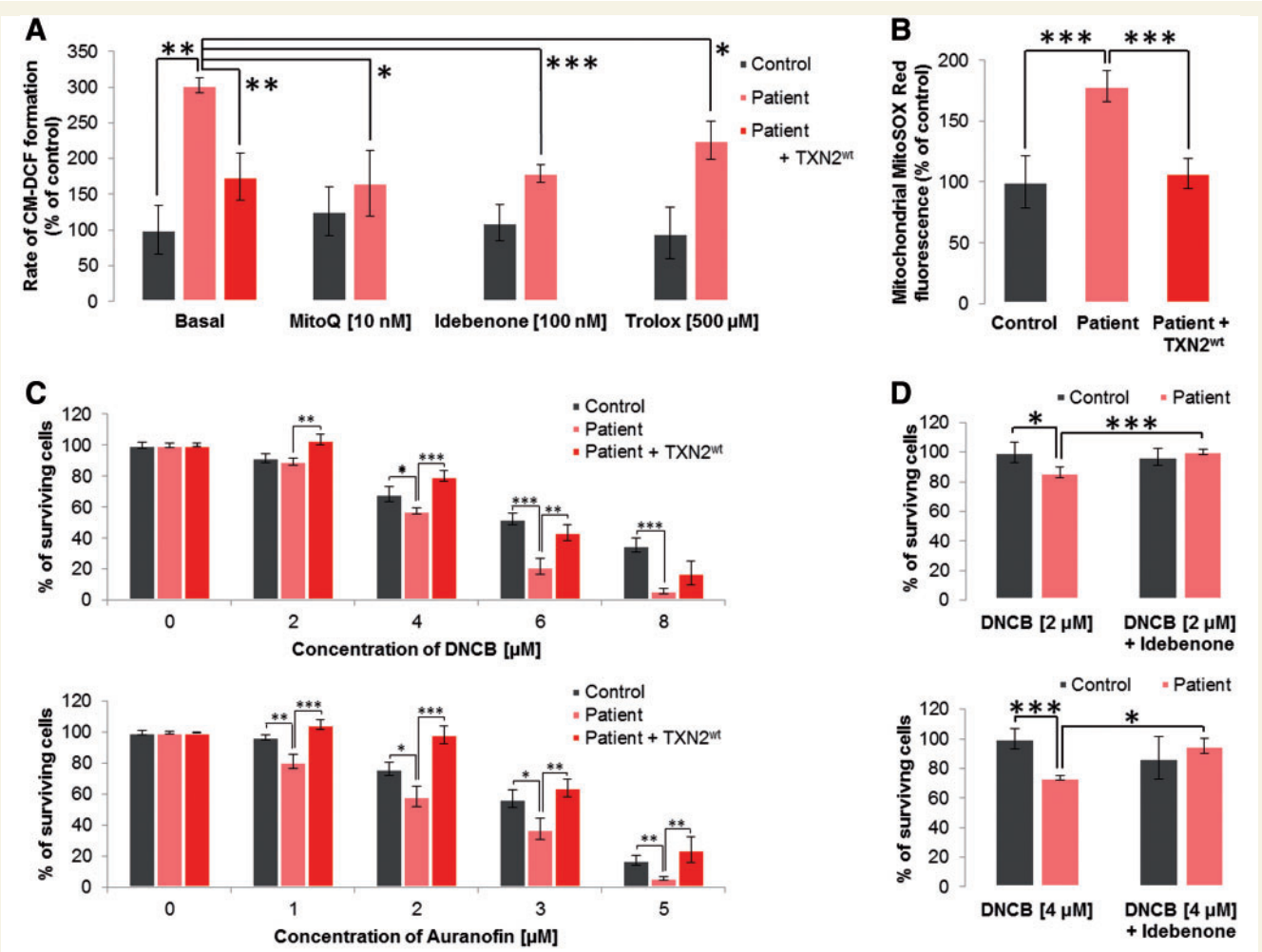

Figure 4 Cellular response to ROS production and scavenging. (**A**) Global cellular ROS levels were determined by using the fluorescent indicator CM-H2DCFA. Patient fibroblasts showed increased ROS levels, which were normalized by re-expression of *TXN2*. Antioxidant treatment (MitoQ, Idebenone and Trolox) reduced ROS levels in patient cells. (**B**) Mitochondrial ROS levels were measured by using the mitochondria-targeted superoxide indicator MitoSOX Red. (**C**) Cell survival assay: cells were treated for 72 h with the indicated concentrations of pharmacological inhibitors. Patient cells were significantly more sensitive to inhibition of the corresponding system glutathione reductase (DCNB; *top*) and TXNRD2 (Auranofin; *bottom*). Re-expression of *TXN2* rescued this phenotype and normalized the survival rate. (**D**) Idebenone (200 nM) furthermore improved cell survival rate in a 72 h assay with different concentration of DNCB (2 and 4 µM, *top* and *bottom*, respectively).

ROS defence metabolism (Fig. 4C). Direct inhibition of the GSH pathway at the GSH reductase level by 2,4-dinitrochlorobenzene (DNCB) showed significantly higher sensitivity of patient cells, which suggests a role of the GSH pathway in partial compensation as well as crosstalk of both pathways. Auranofin as an inhibitor of TXNRD also significantly affected the survival rate of the patient cell line in comparison to the control, indicating an additional action of TXNRD2 on PRDX3 or other parts of the ROS defence system. Importantly, in all assays mentioned above, the abnormal results in patient cells (increased ROS production/enhanced drug sensitivity) were normalized to control values by the re-expression of *TXN2*. Of note, *TXN2* over-expression in control cells did not cause any significant changes (data not shown).

Idebenone improves cell survival and mitigates clinical symptoms

Based on the established defect in ROS regulation, we tested three well-known antioxidants on the cellular level (MitoQ, Idebenone, Trolox) and observed reduced ROS levels in patient fibroblasts (Fig. 4A). In view of clinical availability, we decided to further evaluate the therapeutic potential of Idebenone (a synthetic analogue of coenzyme Q_{10}). As depicted in Fig. 4D, Idebenone treatment rescued TXN2-deficiency mediated DNCB-sensitivity. In view of this finding, we started to treat the patient with Idebenone (900 mg/day) in a compassionate use setting. During a follow-up period of 4 months we noted improved feeding behaviour (less tube feeding required), considerable

weight gain from 39.5 kg body weight [body mass index (BMI) < third percentile] up to 45 kg body (BMI 10th percentile) and increased physical capacity.

Discussion

Mitochondrial oxidative metabolism is essential for neuronal function and survival, although it is inevitably linked to the generation of substantial amounts of ROS (Dringen *et al.*, 2000; Koopman *et al.*, 2013). Accordingly, antioxidant systems play a crucial role within the CNS as exemplified by high levels of TXN2 in brain tissue (Rybnikova *et al.*, 2000; Silva-Adaya *et al.*, 2014). The patient reported here with a null mutation in *TXN2* presented prenatal brain abnormalities (e.g. primary microcephaly, large subependymal cysts, hippocampal malformation). Aggravation of the phenotype was already detectable during the first year of life, manifesting in rapid cerebellar atrophy and global brain atrophy. Later on, retinopathy, optic atrophy, axonal neuropathy and autonomic dysfunction became evident. These findings suggest a critical role for TXN2 for human neurodevelopment and neuronal maintenance. In this context, the cerebellum appears to be specifically vulnerable. Interestingly, inactivation of the cytosolic thioredoxin reductase (TXNRD1) in neural precursor cells was shown to induce massive cerebellar hypoplasia in mice, which additionally suggests a role of the TXN system in cerebellar development (Soerensen *et al.*, 2008).

In comparison with embryonic lethality of the *Txn2* knock-out mouse model (Nonn *et al.*, 2003), it is surprising that the patient reported here is currently 16 years old, indicating additional compensatory mechanisms. Analogously, *Txnrd2* knockout mice die during embryonic development (Conrad *et al.*, 2004), while patients with a loss-of-function mutation in *TXNRD2* are known to survive (Prasad *et al.*, 2014). It has been established that a parallel protective system, the GSH system, is highly effective, which might be of particular relevance in this context (Conrad *et al.*, 2004; Zhang *et al.*, 2007). Moreover, mitochondrial PRDX3 can also be reduced by glutaredoxin 2 (GLRX2) or even TXNRD2 (Hanschmann *et al.*, 2010) (Fig. 1) directly, thus representing possible backup systems for TXN2/GLRX2 in certain tissues (Hanschmann *et al.*, 2010). Our experiments with chemical inhibitors of the GSH system or TXNRD2 indeed demonstrated an increased sensitivity of patient cells, supporting the idea of crosstalk between both pathways.

Importantly, ROS (dys)regulation has critical implications for mitochondrial function and oxidative stress may impair oxidative phosphorylation (Distelmaier *et al.*, 2012). Our genetic data in combination with rescue experiments show that TXN2 deficiency results in increased ROS levels and impaired function of the OXPHOS system leading to reduced ATP availability. This finding is in line with the observation of pharmacological inhibition of the mitochondrial TXN system in endothelial cells leading to lower oxygen consumption, decreased ATP/ADP ratios, and increased lactate formation (Lowes and Galley, 2011). Moreover, TXN2 may regulate mitochondrial bioenergetics by affecting cellular glucose uptake (Yoshioka and Lee, 2014). In addition, TXN2 has been recently shown as a master regulator of the tricarboxylic acid cycle as well as for the entry of electrons into the electron transport chain at complex II in plants (Daloso *et al.*, 2015).

In conclusion, our results might point to a therapeutic potential of early antioxidant supplementation in patients with *TXN2* mutations. Moreover, our report on the first patient with TXN2 deficiency indicates an important role of ROS homeostasis for human neurodevelopment, neuronal maintenance and energy metabolism. Additionally, TXN2 might be an interesting target for further experimental studies of diseases with predominant cerebellar involvement (e.g. spinocerebellar ataxias or multiple system atrophy).

Acknowledgements

We thank the patient and the family for participating in this study. Anti-peroxiredoxin-3 antibody was a kind gift from Dr Lillig, C. H. Institut für Biochemie und Molekularbiologie, Universitätsmedizin Greifswald, Ernst-Moritz-Arndt-Universität, Greifswald, Germany. We acknowledge Prof. Michael Knauth, Institute for Diagnostic and Interventional Neuroradiology, Georg-August University Göttingen, for providing follow-up MRI images. Furthermore, we acknowledge Prof. R. C. A. Sengers, Academisch Ziekenhuis, Radboud University Nijmegen, for biochemical measurements in muscle tissue. The authors would like to thank the Exome Aggregation Consortium and the groups that provided exome variant data for comparison. A full list of contributing groups can be found at http://exac.broadinstitute.org/about.

Funding

This project was supported by the BMBF funded German Network for Mitochondrial Disorders (mitoNET #01GM1113C), by the E-Rare project GENOMIT (01GM1207) and by EU FP7 Mitochondrial European Educational Training project (317433). T.B.H. was supported by the BMBF through the Juniorverbund in der Systemmedizin "mitOmics" (FKZ 01ZX1405C). T.M. was supported by the Deutsche Forschungsgemeinschaft (German Research Foundation) within the framework of the Munich Cluster for Systems Neurology (EXC 1010 SyNergy) as well as by the DZHK (German Centre for Cardiovascular Research) and the BMBF (German Ministry of Education and Research). F.D. was supported by a grant from the Forschungskommission of the Medical Faculty of the Heinrich-Heine-University Düsseldorf.

References

Conrad M, Jakupoglu C, Moreno SG, Lippl S, Banjac A, Schneider M, et al. Essential role for mitochondrial thioredoxin reductase in hematopoiesis, heart development, and heart function. Mol Cell Biol 2004; 24: 9414–23.

Daloso DM, Muller K, Obata T, Florian A, Tohge T, Bottcher A, et al. Thioredoxin, a master regulator of the tricarboxylic acid cycle in plant mitochondria. Proc Natl Acad Sci USA 2015; 112: 2.

Distelmaier F, Valsecchi F, Forkink M, van Emst-de Vries S, Swarts HG, et al. Trolox-sensitive reactive oxygen species regulate mitochondrial morphology, oxidative phosphorylation and cytosolic calcium handling in healthy cells. Antioxid Redox Signal 2012; 17: 1657–69.

Distelmaier F, Valsecchi F, Liemburg-Apers DC, Lebiedzinska M, Rodenburg RJ, Heil S, et al. Mitochondrial dysfunction in primary human fibroblasts triggers an adaptive cell survival program that requires AMPK-alpha. Biochim Biophys Acta 2015; 3: 529–40.

Dringen R, Gutterer JM, Hirrlinger J. Glutathione metabolism in brain metabolic interaction between astrocytes and neurons in the defense against reactive oxygen species. Eur J Biochem 2000; 267: 4912–6.

Godoy JR, Funke M, Ackermann W, Haunhorst P, Oesteritz S, Capani F, et al. Redox atlas of the mouse. Immunohistochemical detection of glutaredoxin-, peroxiredoxin-, and thioredoxin-family proteins in various tissues of the laboratory mouse. Biochim Biophys Acta 2011; 1: 2–92.

Haack TB, Hogarth P, Kruer MC, Gregory A, Wieland T, Schwarzmayr T, et al. Exome sequencing reveals de novo WDR45 mutations causing a phenotypically distinct, X-linked dominant form of NBIA. Am J Hum Genet 2012; 91: 1144–9.

Hanschmann EM, Lonn ME, Schutte LD, Funke M, Godoy JR, Eitner S, et al. Both thioredoxin 2 and glutaredoxin 2 contribute to the reduction of the mitochondrial 2-Cys peroxiredoxin Prx3. J Biol Chem 2010; 285: 40699–705.

Holzerova E, Prokisch H, 2015. Mitochondria: much ado about nothing? How dangerous is reactive oxygen species production? Int J Biochem Cell Biol 2015; 7: 021.

Koopman WJ, Distelmaier F, Smeitink JA, Willems PH. OXPHOS mutations and neurodegeneration. EMBO J 2013; 32: 9–29.

Kornblum C, Nicholls TJ, Haack TB, Scholer S, Peeva V, Danhauser K, et al. Loss-of-function mutations in MGME1 impair mtDNA replication and cause multisystemic mitochondrial disease. Nat Genet 2013; 45: 214–9.

Lowes DA, Galley HF. Mitochondrial protection by the thioredoxin-2 and glutathione systems in an *in vitro* endothelial model of sepsis. Biochem J 2011; 436: 123–32.

Lu J, Holmgren A. Thioredoxin system in cell death progression. Antioxid Redox Signal 2012; 17: 1738–47.

Mahmood DF, Abderrazak A, El Hadri K, Simmet T, Rouis M. The thioredoxin system as a therapeutic target in human health and disease. Antioxid Redox Signal 2013; 19: 1266–303.

Nonn L, Williams RR, Erickson RP, Powis G. The absence of mitochondrial thioredoxin 2 causes massive apoptosis, exencephaly, and early embryonic lethality in homozygous mice. Mol Cell Biol 2003; 23: 916–22.

Prasad R, Chan LF, Hughes CR, Kaski JP, Kowalczyk JC, Savage MO, et al. Thioredoxin reductase 2 (TXNRD2) mutation associated with familial glucocorticoid deficiency (FGD). J Clin Endocrinol Metab 2014; 99: 2013–3844.

Rybnikova E, Damdimopoulos AE, Gustafsson JA, Spyrou G, Pelto-Huikko M. Expression of novel antioxidant thioredoxin-2 in the rat brain. Eur J Neurosci 2000; 12: 1669–78.

Sena LA, Chandel NS. Physiological roles of mitochondrial reactive oxygen species. Mol Cell 2012; 48: 158–67.

Silva-Adaya D, Gonsebatt ME, Guevara J. Thioredoxin system regulation in the central nervous system: experimental models and clinical evidence. Oxid Med Cell Longev 2014; 590808: 27.

Soerensen J, Jakupoglu C, Beck H, Forster H, Schmidt J, Schmahl W, et al. The role of thioredoxin reductases in brain development. PLoS One 2008; 3: 0001813.

Tanaka T, Hosoi F, Yamaguchi-Iwai Y, Nakamura H, Masutani H, Ueda S, et al. Thioredoxin-2 (TRX-2) is an essential gene regulating mitochondria-dependent apoptosis. EMBO J 2002; 21: 1695–703.

Winterbourn CC, Hampton MB. Redox biology: signaling via a peroxiredoxin sensor. Nat Chem Biol 2015; 11: 5–6.

Yoshioka J, Lee RT. Thioredoxin-interacting protein and myocardial mitochondrial function in ischemia-reperfusion injury. Trends Cardiovasc Med 2014; 24: 75–80.

Zhang H, Go YM, Jones DP. Mitochondrial thioredoxin-2/peroxiredoxin-3 system functions in parallel with mitochondrial GSH system in protection against oxidative stress. Arch Biochem Biophys 2007; 465: 119–26.

Zorov DB, Juhaszova M, Sollott SJ. Mitochondrial reactive oxygen species (ROS) and ROS-induced ROS release. Physiol Rev 2014; 94: 909–50.